

First-Order Stochastic Cellular Automata Simulations of the Lindemann Mechanism

CHAD A. HOLLINGSWORTH,¹ PAUL G. SEYBOLD,² LEMONT B. KIER,³ CHAO-KUN CHENG⁴

¹Department of Chemistry, Wright State University, Dayton, Ohio 45435

²Departments of Chemistry and Biochemistry, Wright State University, Dayton, Ohio 45435

³Department of Medicinal Chemistry, Virginia Commonwealth University, Richmond, Virginia 23298

⁴Department of Mathematical Sciences, Virginia Commonwealth University, Richmond, Virginia 23298

Received 12 July 2002; accepted 7 November 2003

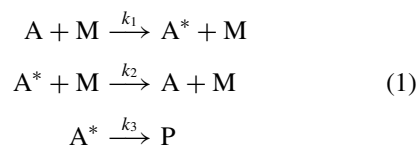
DOI 10.1002/kin.10191

ABSTRACT: The Lindemann mechanism explains how apparent unimolecular chemical reactions arise from bimolecular collisions. In this mechanism an ingredient M activates reactants A through collisions, and the resulting activated species A* can either decay to products P or be deactivated back to A, again via collisions with M. A first-order stochastic cellular automata model described previously [Seybold, Kier, and Cheng, *J Chem Inf Comput Sci* **1997**, *37*, 386] has been modified to simulate this mechanism. It is demonstrated that this model accurately reflects the salient features of the Lindemann mechanism, including the normal second-order kinetic behavior at low [M] and apparent first-order kinetics at high [M]. At low [M] the mechanism is equivalent to a rate-limited sequential process, whereas at high [M] it becomes a preequilibrium with leakage to products. The model also allows an examination of the validity of the steady-state approximation normally employed in a deterministic analysis of this mechanism, and it is seen that this approximation is not well justified under reasonable conditions. © 2004 Wiley Periodicals, Inc. *Int J Chem Kinet* 36: 230–237, 2004

INTRODUCTION

By the early years of the twentieth century a number of gas-phase reactions were known that appeared to be unimolecular, occurring without collisions. Perrin [1] proposed that the reacting molecules were activated by infrared radiation from the reaction vessel walls. Thermodynamic reasoning, however, shows that such a process cannot be responsible for the reactions observed

[2]. Subsequent studies by Lindemann [3], Christiansen [4,5], and Hinshelwood [6] led to a mechanism consisting of three elementary steps involving the reacting species A, a collisionally activated species A*, a collision partner M, and product P:



This set of reactions has come to be called the Lindemann mechanism. In this, conversion of the

Correspondence to: Paul G. Seybold; e-mail: paul.seybold@wright.edu.
© 2004 Wiley Periodicals, Inc.

activated species A^* to product P competes with deactivating collisions of A^* with the species M .

The customary approach to this mechanism and similar kinetic phenomena is to describe the time-dependent changes in the reacting species in terms of a set of coupled differential rate expressions [7,8]:

$$\begin{aligned}\frac{d[A]}{dt} &= k_1[A^*][M] - k_2[M][A] \\ \frac{d[A^*]}{dt} &= -k_1[A^*][M] + k_2[M][A] - k_3[A^*] \quad (2) \\ \frac{d[P]}{dt} &= k_3[A^*]\end{aligned}$$

Usually the *steady-state approximation* $d[A^*]/dt \approx 0$, i.e., that the concentration of the intermediate A^* remains relatively constant over a suitable portion of the reaction time, is applied at this point, leading to an expression for the reaction rate v ,

$$v = \frac{d[P]}{dt} = \frac{k_1 k_3 [A][M]}{k_3 + k_2 [M]} \quad (3)$$

At high pressures of M , $k_2[M] \gg k_3$ and expression (3) reduces to the first-order rate expression $v \approx (k_1 k_3 / k_2)[A]$, whereas at low pressures $k_2[M] \ll k_3$ and $v \approx k_1[A][M]$, the second-order form.

Cellular automata models [9–12] provide an alternative, discrete approach to the traditional differential rate-equation-based approach outlined above. These models are based on concepts first suggested by Ulam [13], von Neumann [14], and Zuse [15,16] a half century ago, and avoid several of the shortcomings of the traditional approach, such as reliance on approximations and failure to account for fluctuations in finite systems. In their underlying mathematical practice they share some features in common with integrated Monte Carlo procedures [17]. The models treat physical and chemical systems as discrete in space and time, and operate under user-defined rules that may be either deterministic or probabilistic. Cellular automata models have been applied to the study of a number of phenomena in physics [10,12,13,18], biology [19], and chemistry [12,13,20–26]. These models represent a *mesoscale* approach [27] to dynamic phenomena in the sense that they stand at a level of detail intermediate between the intimate examination of single species found, e.g., in a quantum mechanical treatment, and the broad-brushed continuous treatment found in the deterministic approach based on the rate equations.

For the past several years we have been examining applications of cellular automata models to dynamic

chemical systems [28–30], and we have recently described a general stochastic cellular automaton model for first-order reaction kinetics [31]. The latter model has served as a basis for simulations of a variety of phenomena, including molecular excited-state dynamics [32,33] and chemical kinetics [34]. In these cellular automata models the rate constants of the traditional approach are replaced by transition probabilities, and because of the probabilistic nature of the transition rules each simulation run is, in effect, an independent “experiment.” The natural fluctuations expected in the behaviors of finite systems emerge in the simulations as variations observed between different runs. The traditional deterministic solutions for the phenomena under consideration appear as limiting cases when very large numbers of ingredients or large numbers of trials are employed.

In this report it will be shown that a first-order cellular automaton model successfully reproduces the characteristics of the Lindemann mechanism in a direct and informative manner. The model provides an analysis of the time variations of the populations of each participating species, and allows an evaluation of the extent to which the steady-state approximation is valid.

METHODS

The basic concepts of the cellular automata kinetic models have been described in detail in earlier reports [30,31], and only a brief overview of these ideas will be given here. Simulations take place on an $n \times m = N$ cell grid, with N' of the cells occupied by user-specified ingredients. In general, these ingredients are free to move about the grid in random walks, constrained by user-defined breaking, joining, and gravitational rules. However, in first-order models movement is irrelevant, and all of the grid cells are normally occupied by independently-acting species which may represent different chemical compounds or different states of a single compound. In order to visualize the dynamic processes the species involved are represented by different colors. Transitions between the species are governed by user-defined probabilistic rules. From a given starting configuration the cellular automata systems evolve in time-steps (“iterations”) during which each ingredient is monitored and permitted to transform to another species according to the assigned transition probabilities. When suitable starting conditions and transition rules are assigned, patterns of behavior (“emergent properties”) arise during the systems’ evolutions, that can be related to physical or chemical phenomena.

A cellular automaton analysis of a collisional process would normally require a second-order kinetics model encompassing both movement and transition rules [Moore, J. P.; Seybold, P. G.; Kier, L. B.; Cheng, C.-K. (to be published), Hollingsworth, C. A.; Seybold, P. G.; Kier, L. B.; Cheng, C.-K. (to be published)], but the special conditions of the Lindemann mechanism allow an attractive simplification and the use of a first-order kinetics model with only transition rules in operation. The rates of the first two reactions in mechanism (1), for activation of A to A* and deactivation of A* back to A, depend in an identical manner on the concentration of the colliding species M:

$$\text{Rate}_1 = k_1[A][M]$$

$$\text{Rate}_2 = k_2[A^*][M]$$

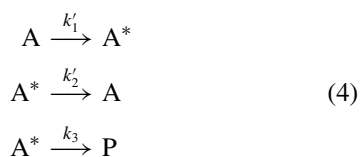
Accordingly, it is convenient to introduce the pseudo first-order rate constants $k'_1 = k_1[M]$ and $k'_2 = k_2[M]$ for these processes, so that the above rate expressions become

$$\text{Rate}_1 = k'_1[A]$$

$$\text{Rate}_2 = k'_2[A^*]$$

This measure also defines the effective activation/deactivation equilibrium constant $K = k'_1/k'_2 = k_1/k_2$. (Note that in the cellular automata models the rate constants k_i are expressed as transition probabilities per iteration.)

With the above restatement, mechanism (1) reduces to a set of first-order reactions



The competition between deactivation of the intermediate A* and product formation is then defined by the ratio $\alpha = k'_2/k_3$. If the inherent second-order rate constants k_1 , k_2 , and k_3 of the reaction are initially established for a particular system, the ratio α is proportional to the pressure [M], since $\alpha = (k_2/k_3)[M]$. Thus the effect of varying [M], the key variable in the Lindemann mechanism, can be simulated by varying the value of k'_1 (and with it $k'_2 = Kk'_1$) while keeping k_3 and the established ratio $K = k_1/k_2$ constant. As noted above, in cellular automata models the rate constants of the traditional deterministic treatment are replaced by corresponding transition probabilities. Hence in a cellular automaton model, simultaneously reducing the transition probabilities k'_1 and k'_2 (while keeping their

ratio $K = k'_2/k'_1$ constant) corresponds to a reduction in [M], and increasing these probabilities simulates an increase in [M]. All of the simulations were carried out on a $100 \times 100 = 10,000$ cell grid, starting with all 10,000 ingredients in form A. Initial reaction rates $v_{\text{init}} = d[P]/dt$, were defined in terms of an appropriate early linear portion in a plot of [P] vs time (t in iterations), and were determined as averages of three simulations for each condition α . In examining the simulations it was observed that an induction period, sometimes brief, preceded the establishment of linear dependence in all cases. At low values of [M], when the rates $k'_1 = k_1[M]$ and $k'_2 = k_2[M]$ were quite small, this period corresponded to the time required for establishment of a steady-state condition. At high [M], where both k'_1 and k'_2 were large, this period corresponded to the relatively brief time (a few iterations) required for establishment of the pseudo-equilibrium between species A and A*. The extent of the induction periods was longest under intermediate conditions, where it could encompass 200–300 iterations.

RESULTS AND DISCUSSION

In order to examine the effect of the *pseudo*-equilibrium constant K on the results, two sets of runs were carried out, the first with $K = 0.5$ and the second with $K = 0.2$. In all cases the first-order A* product formation probability k_3 was held at 0.01/iteration. This allowed both of the extremes $k'_2 \gg k_3$ and $k'_2 \ll k_3$ to be examined. All runs started with all 10,000 cells in the A state. The k'_2 values were systematically varied from 0.99 to 0.00001 in separate runs. (Note that in the highest [M] case the choice $k'_2 = 1.00$ would have required $k_3 = 0.0$, so that no product would be produced. Hence k'_2 was assigned as 0.99 to accommodate $k_3 = 0.01$.) The parameter values tested are shown in Table I.

Case I: $K = 0.5$

An illustration of the early simulation period for the case $k'_1 = 0.0005$ and $k'_2 = 0.001$, showing the induction period and the establishment of the linear initial rate period, is given in Fig. 1. The rate data for the different parameter values are summarized in Table I. The results show that the initial linear product production rates $v = d[P]/dt$ remain reasonably steady so long as $k'_2 \geq \sim 10k_3$, but those beyond that point fall steadily as k'_2 is decreased. The uncertainties in the initial rates correspond to standard deviations obtained from three trial runs. (Note that these uncertainties would be greater

Table I Transition Probabilities and Resulting Initial Reaction Rates $d[P]/dt$. In All Cases $k_3 = 0.01$. The Uncertainties Were Obtained from Three Trials

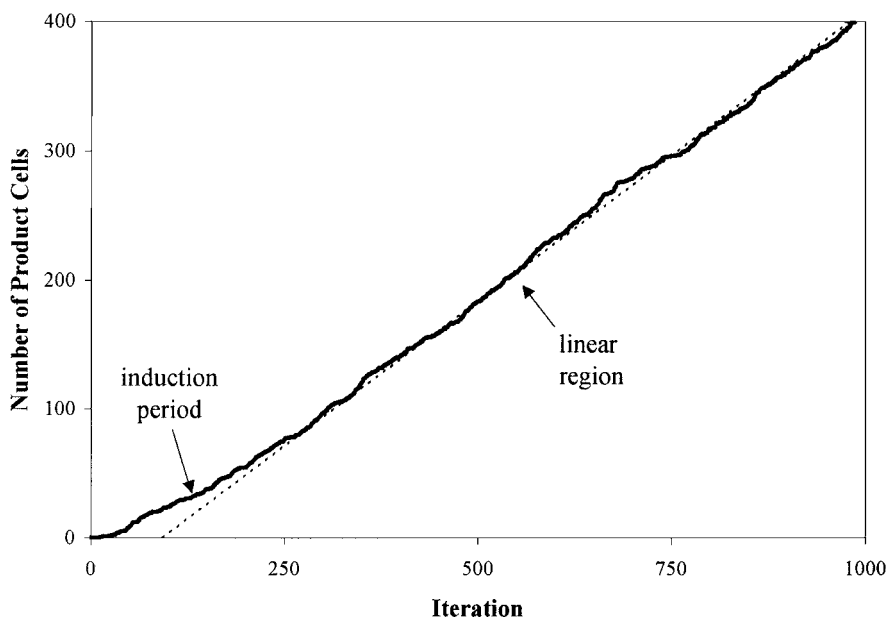
$K = 0.5$			$K = 0.2$		
k'_1	k'_2	$d[P]/dt$	k'_1	k'_2	$d[P]/dt$
0.5	0.99	28.83 ± 0.11	0.2	0.99	15.29 ± 0.05
0.25	0.5	28.74 ± 0.07	0.1	0.5	14.71 ± 0.04
0.05	0.1	26.41 ± 0.06	0.02	0.1	14.81 ± 0.031
0.01	0.02	21.69 ± 0.09	0.002	0.01	8.003 ± 0.007
0.005	0.01	16.55 ± 0.06	0.0002	0.001	1.725 ± 0.001
0.0005	0.001	3.953 ± 0.008	0.00004	0.0002	0.4076 ± 0.0003
0.0001	0.0002	0.9105 ± 0.0004	0.00002	0.0001	0.1909 ± 0.0000
0.00005	0.0001	0.4523 ± 0.0001	0.000002	0.00001	0.0201 ± 0.0000
0.000005	0.00001	0.0479 ± 0.0000	–	–	–

if fewer cells, e.g., $N' = 1000$, were employed in the simulations.)

A plot of the variations in the populations of the species A, A*, and P for the intermediate case $k'_1 = 0.005$, $k'_2 = 0.01$, and $k_3 = 0.01$ is shown in Fig. 2. It is apparent that the concentration of the intermediate A* first rises to a peak, and then falls off steadily as the simulation progresses. We note that this result is in contrast to the customary steady-state assumption that the intermediate concentration should be relatively constant as the reaction proceeds. (Forst [35] has noted that generally the steady-state solution works well under “coarse” time resolution, but not under “fine” time resolution.) This plot is typi-

cal of the overall shapes of the population changes for different cases, although the timeframe for the observed variations became substantially longer as the rates k'_1 and k'_2 were decreased to simulate a decrease in [M].

The data in Table I allow us to plot the variations in the initial rates ($d[P]/dt$) against the implied values of [M] obtained from the k'_2 values. This plot is shown in logarithmic form in Fig. 3, and is seen to resemble typical experimental plots for such reactions (e.g., the thermal isomerization of methyl isocyanide [36] or the thermal isomerization of cyclopropane [37]). An initial linear dependence on [M] at low [M] converts to a later portion of the curve at high [M] in which the initial

**Figure 1** Early formation of product P for the case $K = 0.5$, $k'_1 = 0.00005$, and $k'_2 = 0.0001$.

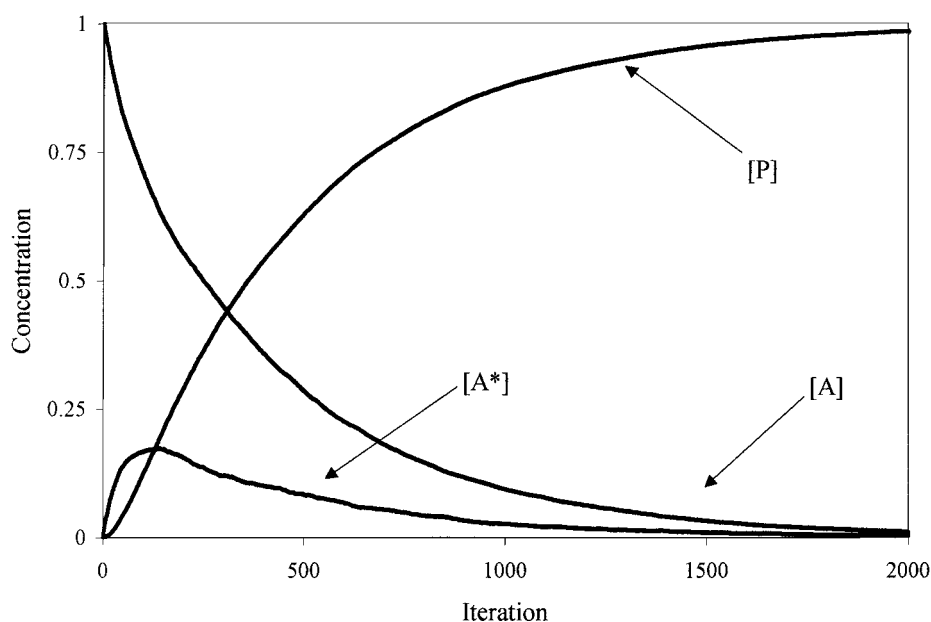


Figure 2 Plot of the variations in the species concentrations for the case $K = 0.5$, $k'_2 = 0.01$, and $k'_1 = 0.005$.

rate is independent of $[M]$; these portions of the curve correspond to a traditional second-order dependence and an apparent first-order (unimolecular) dependence, respectively.

For large $[M]$ $k'_2 \gg k_3$, deactivation of A^* to A dominates over decay to products, and a preequilibrium condition prevails. When $[M]$ is small k'_2 can be neglected compared to k_3 , and expressions (4) reduce to the sequential steps $A \rightarrow A^* \rightarrow P$.

Case II: $K = 0.2$

The results for the simulations carried out with $K = 0.2$ were qualitatively quite similar to those for $K = 0.5$. As above, k_3 was held constant at 0.01 for all the simulations. The early stages of the simulation for $k'_1 = 0.00002$ and $k'_2 = 0.0001$ is illustrated in Fig. 4, and shows the induction period and start of the linear dependence for this case. The initial linear rates of buildup

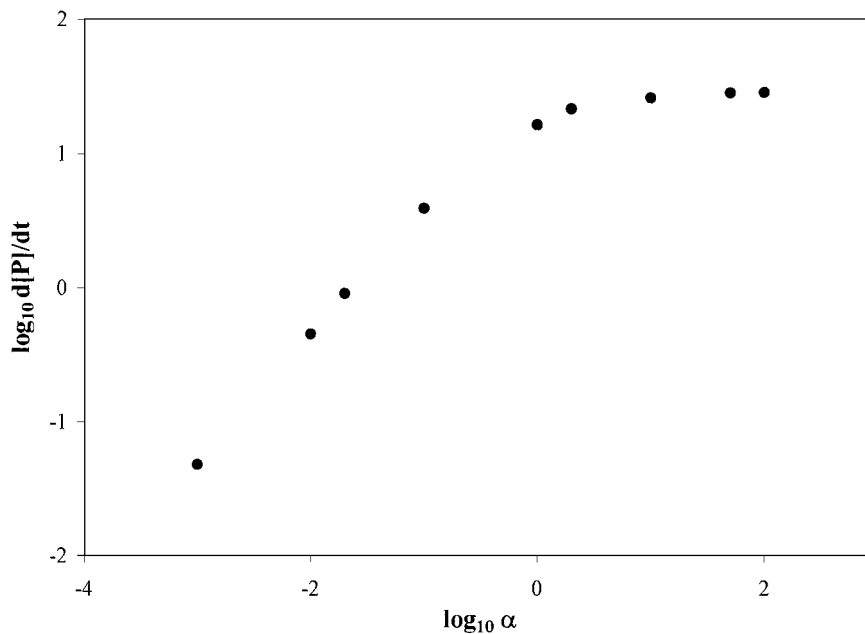


Figure 3 Plot of the initial reaction rates $d[P]/dt$ vs α (where α is proportional to the concentration of the collision partner species M) for the case $K = 0.5$.

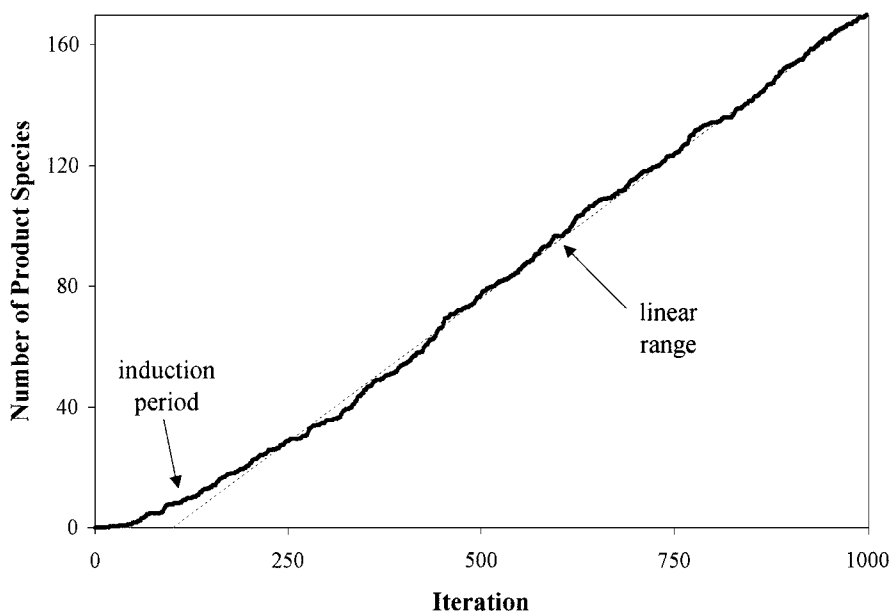


Figure 4 Early formation of product P for the case $K = 0.2$, $k_1' = 0.00002$, and $k_2' = 0.0001$.

of P for all the cases examined are given in Table I. The variations in the concentrations of A, A^* , and P for the case $k_1' = 0.005$, $k_2' = 0.01$ are shown in Fig. 5. A plot of these rates vs α is shown in Fig. 6. As before, this latter curve shows the transition from typical second-order kinetic behavior at low [M] (low α) to apparent first-order kinetic behavior at high [M] (high α).

As in the $K = 0.5$ case, the concentration of the intermediate A^* is seen to first rise, then fall steadily, in

contrast to the roughly constant value for $[A^*]$ assumed in the steady-state approximation of deterministic kinetic theory. Apparently the deterministic solution is sufficiently insensitive to the variations in $[A^*]$ to allow a fairly accurate picture of the mechanism to emerge despite the inaccuracy of the steady-state assumption. In any case, the cellular automata models require no such assumption and portray the variations in concentration directly as they occur in the mechanism.

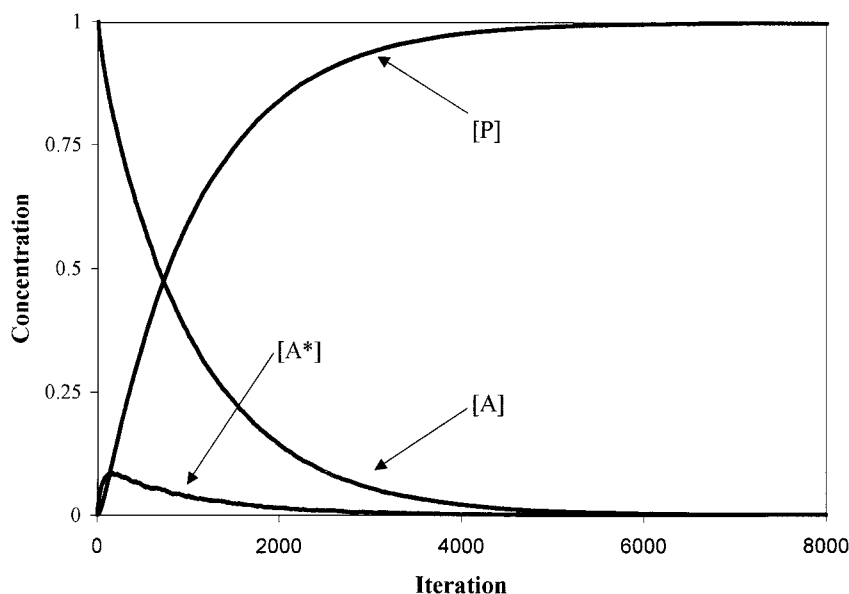


Figure 5 Plot of the variations in the species concentrations for the case $K = 0.2$, $k_1' = 0.005$, and $k_2' = 0.01$.

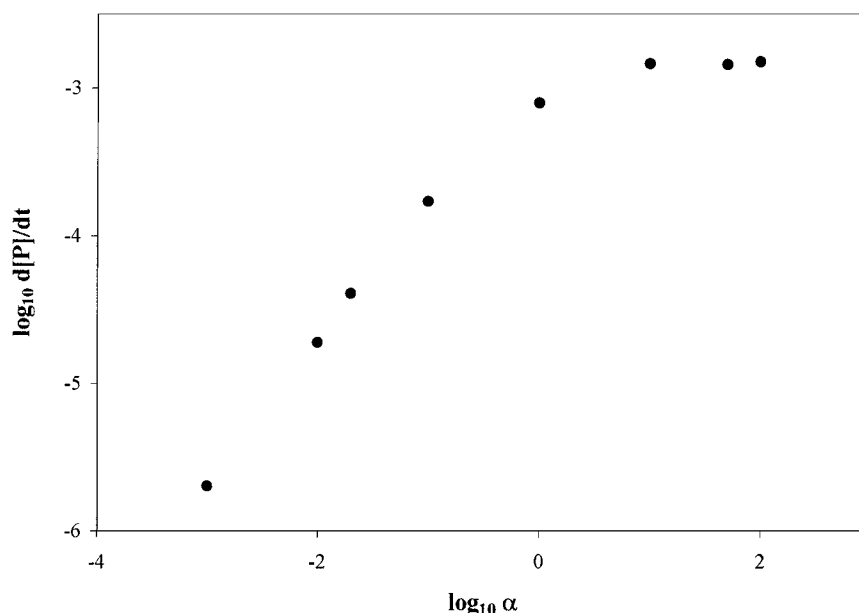


Figure 6 Plot of the logarithms of the initial reaction rates $d[P]/dt$ vs α (where α is proportional to the concentration of the collision partner species M) for the case $K = 0.2$.

CONCLUSIONS

It has been demonstrated that a first-order cellular automaton model provides an insightful and accurate portrayal of the classic Lindemann mechanism. The simulations display the transition from second-order to apparent first-order kinetic behavior that occurs when the effective concentration of an inert collision partner species M is increased from a very low value to a high value, thereby affecting the relative rates of the deactivation and product-forming reactions for the intermediate species A^* . It is seen that at low $[M]$ the reaction $A \rightarrow P$ proceeds as a typical two-step process $A \rightarrow A^* \rightarrow P$, with the first step as the rate-limiting step. At high $[M]$ the process has the form of a pre-equilibrium $A \leftrightarrow A^*$ subject to a leakage reaction $A^* \rightarrow P$ [8]. The model is rule-based and the observed behaviors emerge in a natural way without resort to assumptions about the behavior of the intermediate species A^* or other approximations. The results show that the customary deterministic steady-state approximation that $[A^*] \approx \text{constant}$ does not hold up well in the present application. Finally, information on the fluctuations in the species behaviors expected for finite samples can be obtained from repeated simulations.

The authors thank Dr. David Dolson for helpful discussions related to this topic.

BIBLIOGRAPHY

1. Perrin, J. *Ann Phys (Paris)* 1919, 11, 1–108.
2. Steinfeld, J. I.; Francisco, J. S.; Hase, W. I. *Chemical Kinetics and Dynamics*; Prentice-Hall: Englewood Cliffs, NJ, 1989; pp. 352ff.
3. Lindemann, F. A. *Trans Faraday Soc* 1922, 17, 598–599.
4. Christiansen, J. A. PhD thesis, University of Copenhagen, 1921.
5. Christiansen, J. A.; Kramers, H. A. *Zeit Phys Chem* 1923, 104, 451–471.
6. Hinshelwood, C. N. *Proc R Soc A* 1927, 113, 230–233.
7. Alberty, R. A.; Silbey, R. J. *Physical Chemistry*, 2nd ed.; Wiley: New York, 1997; pp. 648–651.
8. Atkins, P. *Physical Chemistry*, 6th ed.; Freeman: New York, 1998; pp. 782–785.
9. Toffoli, T.; Margolus, N. *Cellular Automata Machines. A New Environment for Modeling*; MIT Press: Cambridge, MA, 1987.
10. Wolfram, S. *Cellular Automata and Complexity*; Perseus Press: New York, 1994.
11. Kapral, R.; Showalter, K. (Eds.); *Chemical Waves and Patterns*; Kluwer: Amsterdam, 1995.
12. Chopard, B.; Droz, M. *Cellular Automata Modeling of Physical Systems*; Cambridge University Press: New York, 1998.
13. Ulam, S. M. *Proc Int Congr Math (held in 1950)* 1952, 2, 264.
14. Von Neumann, J. *Theory of Self-Reproducing Automata*; Burks, A. (Ed.); University of Illinois Press: New York, 1966.

15. Zuse, K. *Int J Theor Phys* 1982, 21, 589–600.
16. Schroeder, M. *Fractals, Chaos, Power Laws*; Freeman: New York, 1991; Ch. 17, p. 371.
17. Schaad, L. J. *J Amer Chem Soc* 1963, 85, 3588–3592.
18. Boghosian, B. M. *Comp Phys* 1991, 5, 585–590.
19. Ermentrout, G. B.; Edelstein-Keshet, L. *J Theor Biol* 1993, 160, 97–133.
20. Markus, M.; Hess, B. *Nature* 1990, 347, 56–58.
21. Kapral, R.; Wu, X.-G. *J Phys Chem* 1996, 100, 18976–18985.
22. (a) Vanag, V. K. *J Phys Chem* 1996, 100, 11336–11345; (b) *J Phys Chem* 1997, 101, 7074–7084.
23. Chopard, B.; Droz, M. *Europhys Lett* 1991, 15, 459–465.
24. Cornell, S.; Droz, M.; Chopard, B. *Phys Rev A* 1991, 44, 4826–4812.
25. Cornell, S.; Droz, M.; Chopard, B. *Physica A* 1992, 188, 322–336.
26. Berryman, H. S.; Franceschetti, D. R. *Phys Lett A* 1989, 136, 348–352.
27. Nguyen, S. T.; Gin, D. L.; Hupp, J. T.; Zhang, X. *Proc Natl Acad Sci (USA)* 2001, 98, 11849–11850.
28. (a) Kier, L. B.; Cheng, C.-K. *J Chem Inf Comput Sci* 1994, 34, 647–652; (b) *J Chem Inf Comput Sci* 1994, 34, 1334–1337.
29. Kier, L. B.; Cheng, C.-K.; Seybold, P. G. *SAR and QSAR in Environ Res* 2000, 11, 79–102.
30. Kier, L. B.; Seybold, P. G.; Cheng, C.-K. In *Reviews in Computational Chemistry*; Lipkowitz, K. B.; Boyd, D. (Eds.); Wiley-VCH: New York, 2001; Vol. 17, Ch. 4, pp. 205–254.
31. Seybold, P. G.; Kier, L. B.; Cheng, C.-K. *J Chem Inf Comput Sci* 1997, 37, 386–391.
32. Seybold, P. G.; Kier, L. B.; Cheng, C.-K. *J Phys Chem A* 1998, 102, 886–891.
33. Seybold, P. G.; Kier, L. B.; Cheng, C.-K. *Int J Quantum Chem* 1999, 75, 751–756.
34. Neuforth, A.; Seybold, P. G.; Kier, L. B.; Cheng, C.-K. *Int J Chem Kinet* 2000, 32, 529–534.
35. Forst, W. *Theory of Unimolecular Reactions*; Academic Press: New York, 1973; p. 150.
36. Schneider, P. W.; Rabinowitch, B. S. *J Am Chem Soc* 1962, 84, 4215–4230.
37. Pritchard, H. O.; Sowden, R. D.; Trotman-Dickenson, A. F. *Proc R Soc A (London)* 1953, 217, 563–571.